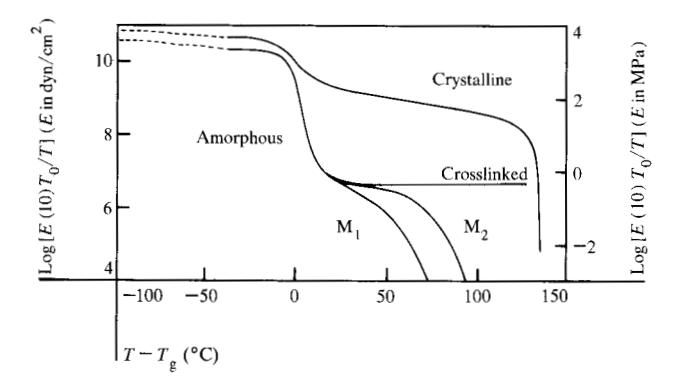
Strength and Related Properties of Elastomeric Block Copolymers

Abstract: Stress-strain curves of single-phase noncrystallizable elastomers over extended ranges of temperature and extension rate are considered qualitatively along with phenomenological and mechanistic aspects of fracture. Data are presented to show that single-phase noncrystallizable elastomers lack toughness except when segmental mobility is sufficiently low so that viscoelastic processes near the tip of a slowly growing crack effectively retard its growth. Highly effective strengthening mechanisms are imparted by plastic domains which result from phase separation in elastomeric block copolymers and from strain-induced crystallization in certain elastomers. The stiffness, tensile strength, and extensibility of a poly(urea-urethane) and three polyurethane elastomers over a broad temperature range are discussed in terms of the type, size, and concentration of the domain-forming segments. These elastomers, and particularly their true stress-at-break, are compared with other block copolymers and with polyurethane elastomers devoid of plastic domains.

Introduction

The mechanical properties of polymers are more highly diverse than those of any other class of materials. Depending on temperature and other test conditions, the response of a particular polymer to stress can be like that of a glass, a soft plastic or leathery material, a rubberlike solid, or an elastic liquid. This diversity of properties [1, 2] is illustrated by the curves in Fig. 1, where the ten-second stress-relaxation modulus (reduced by T_0/T , a ratio of absolute temperatures) is plotted semi-logarithmically against the difference between the test temperature T and the glass temperature T_g . The modulus is measured by suddenly imposing a small constant strain on a specimen and monitoring the retractive force

Figure 1 Schematic representation of the dependence of the ten-second stress-relaxation modulus on the difference between the test temperature and the glass temperature (after Tobolosky [1]).



under isothermal conditions. The tensile stress after ten seconds divided by the strain is the modulus and is denoted by E(10).

At low temperatures this modulus is high, which is characteristic of a glass. With a progressive increase in temperature, the modulus first decreases slowly, then rapidly by a factor of about 1000 in a narrow range above T_{g} , whereupon it becomes nearly constant. Now, if the flow of the polymer is precluded by intermolecular tie-points, e.g., cross-linkages, the modulus increases virtually in direct proportion to the absolute temperature [1, 3-5]. (This behavior is illustrated only implicitly in Fig. 1 because the reduced modulus $E(10)T_0/T$ is shown.) When cross-linkages are absent, internal flow occurs in a specimen at fixed strain and the modulus decays rapidly toward zero. This terminal decay begins at a temperature that increases with the molecular weight of the polymer (cf. M₁ and M₂ in Fig. 1). The modulus of a semicrystalline polymer depends on the morphology and volume fraction of the crystalline phase. Near the crystalline melting point, the modulus drops precipitously.

These changes in mechanical response, except those associated with crystal melting and changes in morphology, occur because molecular motions are retarded by a viscous resistance that depends strongly on temperature, especially near and somewhat above $T_{\rm g}$. It thus follows that the stress in a deformed specimen is time dependent. In principle, the variations depicted in Fig. 1 for amorphous polymers also occur at a single temperature, provided the observational period is sufficiently broad.

154

Thus the mechanical properties depend on both the experimental time scale and the mobility of macromolecular segments, the latter depending on temperature and the nature of the polymer. As a useful though imprecise approximation, different polymers can be considered to be in corresponding states at equal values of $T-T_{\rm g}$, the parameter on the abscissa in Fig. 1.

In a cross-linked (infinite network) polymer at high temperature, the viscous resistance to segmental motions is negligible. Consequently, the stress-strain behavior is usually time independent, i.e., elastic instead of viscoelastic. This elasticity results from the thermal agitation of the chains, intermolecular forces being essentially inconsequential. The elastic and thermoelastic properties of such network polymers are accounted for by the molecular theory of rubber elasticity [1, 3-5].

A polymer that is not cross-linked flows at an elevated temperature. When the molecular weight is high, the viscosity is very high because physical couplings (entanglements) exist among the molecules. During flow, elastic energy is stored and normal stresses develop. These elastic characteristics arise because the random-coil configurations of the molecules are perturbed. When the applied stress is removed, the molecules return to their unperturbed configurations at a rate dependent on segmental mobility, and thereby the specimen recovers in some degree. Thus the polymer is aptly termed an elastic liquid.

As indicated by these introductory remarks, the mechanical properties of a polymer depend strongly on temperature and time (more precisely, on stress or strain history) because of the dominant role played by segmental mobility. Also, most polymers, whether crosslinked or not, are rubberlike under certain conditions. The discussion henceforth is devoted to elastomers, which are amorphous polymers above $T_{\rm g}$ in which viscous flow is prevented by cross-linkages or impeded by colloidal plastic domains.

In the sections that follow, qualitative considerations are first given to: a) the molecular and supermolecular structure of different types of elastomers, b) the stressstrain behavior of single-phase noncrystallizable elastomers over extended ranges of temperature and extension rate, and c) phenomenological and mechanistic aspects of fracture. Then data are reviewed to show that all elastomers composed solely of mobile molecular chains lack toughness. The focus thereafter is on tough elastomers. which contain a dispersed phase. The stiffness and especially the strength and extensibility of recently studied polyurethane and poly(urea-urethane) elastomers that contain innate plastic domains are considered in light of their supermolecular structures. Finally, their strengths are compared with those of other elastomeric block copolymers.

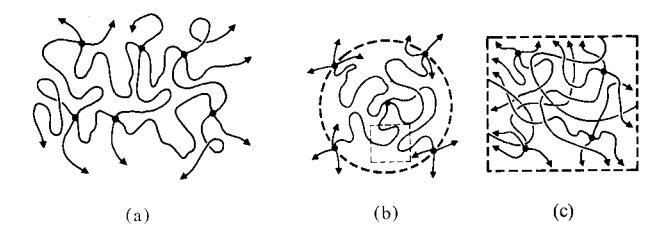


Figure 2 Sketch (a) represents a network polymer. Circles depict network junctions; arrowheads connote that the chains terminate in junctions. This representation is imprecise because junctions that are topological neighbors are usually not spatial neighbors. Figure 2(b) shows a junction and its four topological neighbors. Figure 2(c) represents chains and junctions that reside in the volume element indicated in Fig. 2(b). These junctions are spatial neighbors but are remotely related topologically.

Structure of elastomers

Elastomers are commonly prepared by converting linear macromolecules into a reticular structure through the introduction of sparse cross-linkages [6]. When chemical agents are used, the cross-linking process, termed vulcanization, yields a rubber vulcanizate whose network structure is depicted in Fig. 2(a). The black dots denote cross-linkages (i.e., chain junctions). The molecular weight of a network chain, which is a macrosegment that extends between two junctions, is typically between 5000 and 10000.

Figure 2(a) is somewhat misleading, however; Fig. 2(b) is a better representation of a network. Four chains are depicted which emanate from a junction centered in a hypothetical sphere and terminate in junctions placed on the surface of the sphere. These chains occupy only a small fraction of the volume; the remainder is filled with other chains and junctions, depicted in the enlarged volume element Fig. 2(c). If the molecular weight of chains is 10000, it can be shown [5] that the sphere typically contains some 50 junctions and the 100 associated chains. Thus, junctions that are spatial neighbors are only remotely related topologically, because of the high degree of interpenetration of network elements. This interpenetration gives rise to chain entanglements that function somewhat as junctions, albeit transient ones, and affect the mechanical properties of elastomers and other polymeric materials as well [2]. For example, the plateau of the curves in Fig. 1 for the uncross-linked amorphous polymers in the rubberlike response region arises from entanglements.

Certain elastomers, exemplified by a natural rubber vulcanizate, crystallize rapidly when stretched several hundred percent [3]. The crystalline domains thus generated impart high strength and toughness. Carbon black or other particulate filler is commonly incorporated in an elastomer to increase its stiffness and, in certain instances, its toughness.

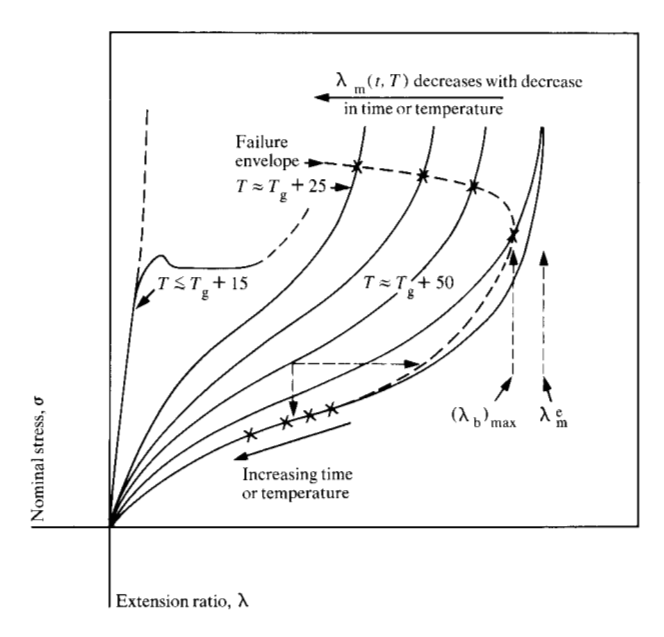


Figure 3 Schematic illustration of the time- and temperature-dependence of stress-strain curves, the maximum extensibility $\lambda_{\rm m}(t,T)$, and the stress and deformation at fracture.

The chemical structure and morphology of elastomeric block copolymers [7] differ from those of conventional elastomers. Each molecule is composed of two or more dissimilar types of macrosegments coupled by chemical bonds. In the polyurethane and poly(ureaurethane) elastomers discussed subsequently, a molecule consists of a number of relatively short segments of rather high polarity, termed "hard" segments, each attached between long segments of low polarity, termed "soft" segments. As a consequence of phase separation, the undiluted copolymer contains submicron clusters of hard segments dispersed in a rubbery matrix of soft segments. The clusters, which may be amorphous, paracrystalline, or crystalline, have a high softening or melting temperature and therefore are termed plastic domains. Such domains serve as multifunctional junctions that impede viscous flow and thus impart elastomeric characteristics to the material. Because flow can occur above the softening temperature of the domains, a block copolymer can be processed as a thermoplastic, provided chemical degradation does not occur at the requisite temperature.

The properties of elastomers considered here are primarily strength and extensibility. For elastomers, unlike rigid materials, these ultimate mechanical properties provide a reasonably good measure of toughness, or the resistance to crack growth. The subject of toughness is introduced through a discussion of elastomers that are devoid of particulate filler and plastic domains, either innate or resulting from crystallization under strain.

Because such single-phase noncrystallizable elastomers lack toughness, they are of limited technological importance. Nevertheless, the concepts derived from studies of such elastomers are essential to an understanding of the properties of tough elastomers, all of which owe their strength to a dispersed phase. The tough elastomers considered are block copolymers; other types are discussed elsewhere [8].

Tensile properties of single-phase noncrystallizable elastomers

The strength and extensibility of an elastomer depend on its global viscoelastic properties, which are reflected in the time and temperature dependence of stress-strain curves, and also on those discrete processes, including crack formation and growth, that culminate in high-speed crack propagation. Because fracture is the terminus of a stress-strain curve, most factors that affect such curves are relevant to concepts about strength, extensibility, and the fracture process.

• Stress-strain curves

Single-phase noncrystallizable elastomers are exemplified by an unfilled styrene-butadiene rubber (SBR) vulcanizate. To view their viscoelastic and strength characteristics generally, imagine first that fracture occurs only under a very high (essentially infinite) stress. Stressstrain curves measured over a broad temperature range would then resemble those sketched in Fig. 3. The coordinates are the engineering or nominal stress σ (load per unit initial area) and the extension ratio λ (length of the stretched specimen per unit initial length). Conceptually, the curves result from tests made either at a fixed extension rate at various temperatures or at different extension rates under isothermal conditions. Moving from right to left in Fig. 3 corresponds to a reduction in either temperature or time; the time equals $(\lambda - 1)/\dot{\lambda}$, where $\dot{\lambda}$ is the extension rate. The curve on the right represents elastic or equilibrium (time independent) behavior. Departures from equilibrium result from a slow stress-biased diffusion of network chains toward equilibrium configurations commensurate with the extant deformation. During any test, the stress increases rapidly toward infinity as λ approaches the maximum extensibility, $\lambda_m(t, T)$. This time- and temperature-dependent parameter, which cannot be measured directly, is basic to the understanding of viscoelastic phenomena at large deformations, especially at temperatures below about $T_u + 50^{\circ}\text{C}$ [9–12].

Data on an SBR vulcanizate in equibiaxial tension show clearly that $\lambda_{\rm m}$ is independent of time and temperature at $T \gtrsim T_{\rm g} + 50^{\circ}{\rm C}$ [11], denoted therefore by $\lambda_{\rm m}^e$. (In simple tension, this is possibly only approximately true [10, 12].) At lower temperatures, $\lambda_{\rm m}$ decreases

rapidly with a reduction in either temperature or time. Depending on segmental mobility and the extension rate, a single network chain may respond as two, three, or more shorter chains [9, 13], thereby reducing λ_m for the network [12]. Because of the very low segmental mobility in the vicinity of T_g , λ_m exceeds unity only slightly when the time equals one minute at such a temperature. The rapid increase in λ_m with time apparently gives rise to the maximum (tensile yielding) commonly observed in stress-strain curves at temperatures near and somewhat above T_g [12], as is illustrated by the curve on the left in Fig. 3. (At temperatures significantly below T_g , yield phenomena unquestionably result from, or are controlled by, a different mechanism.)

• Fracture process and illustrative data

Fracture always terminates the curves in Fig. 3 before $\lambda_{\rm m}$ is attained. The dashed curve, which connects the fracture points, is termed the *failure envelope* [8]. With decreasing temperature or time, the point of fracture traverses the envelope counterclockwise. The extremum occurs at $(\lambda_{\rm b})_{\rm max}$, the maximum extension ratio attainable. Upon deriving the (hypothetical) equilibrium stress-strain curve from time- and temperature-dependent data and the equilibrium modulus [8, 10, 11], it is found that $(\lambda_{\rm b})_{\rm max} < \lambda_{\rm m}^e$. The dashed lines extending from point A serve to illustrate that a specimen maintained either at a constant extension or under a constant load can exhibit delayed fracture [8].

When an elastomer is deformed, microcracks are considered to develop and grow slowly. Eventually some crack becomes unstable and propagates catastrophically. The rate of crack growth prior to catastrophic propagation, and thus the lifetime of a specimen, depends on the dissipation of elastic energy near the crack tip through viscoelastic processes associated with crack enlargement [13-15]. This impediment to crack growth, arising from viscous effects, is in large measure responsible for the strength of noncrystallizable elastomers devoid of plastic domains. It accounts for the marked dependence of the tensile strength $\sigma_{\rm b}$ (based on the initial cross-section of a specimen) and the ultimate extension ratio λ_h on temperature and extension rate, or on deformation history more generally. The fraction of the strength that results from the network per se is small, and is actually negligible in many instances (see the Summary).

Because viscoelastic processes play a dominant role, values of σ_b and λ_b measured at various temperatures and extension rates can be superposed to yield master curves [8, 16]. Each curve is a function of the reduced extension rate λa_T , or reduced time-to-break t_b/a_T , in which the temperature function a_T accounts for the temperature dependence of segmental mobility or "internal" viscosity [2]. It follows that a plot of $\log \sigma_b T_0/T$ vs \log

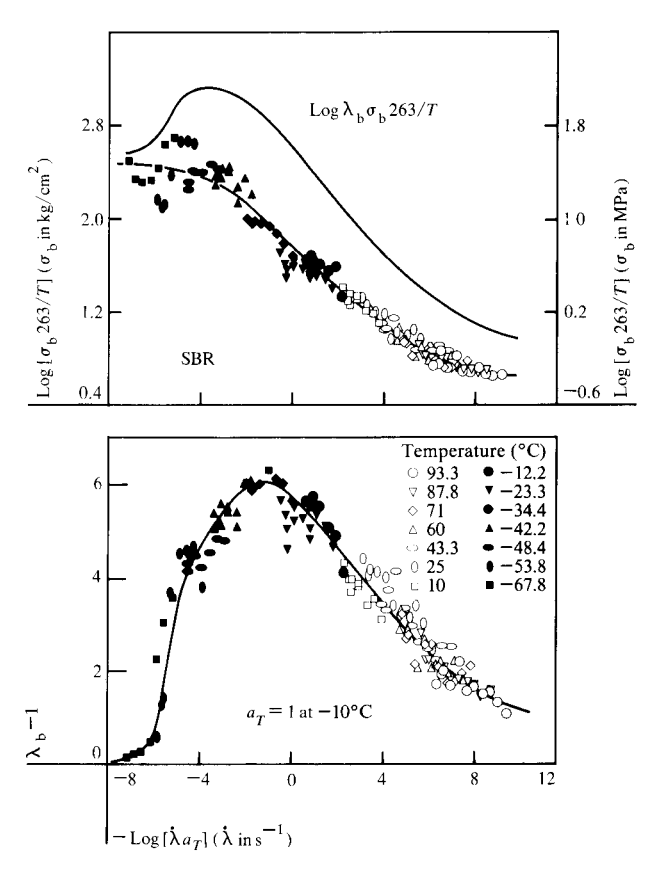


Figure 4 Ultimate tensile properties measured at various extension rates and temperatures on an unfilled styrene-butadiene rubber vulcanizate. Data at the different temperatures have been superposed to yield composite curves [8, 16].

 $(\lambda_b - 1)$, or other measures of the stress and deformation at fracture, will produce a single time- and temperature-independent curve, i.e., the failure envelope. Values of $\sigma_{\rm b}$ are multiplied by $T_{\rm o}/T$, where $T_{\rm o}$ and T are a reference temperature and the test temperature, respectively, expressed in K, in conformity with one step in the time-temperature reduction procedure [1, 2] used to interrelate viscoelastic properties measured at different temperatures. The ratio T_0/T corrects for the fact that the elastic retractive force in a rubbery material increases essentially in direct proportion to the absolute temperature. If the ratio is omitted in preparing a plot of $\log \sigma_{\rm b} T_{\rm o} / T$ vs $\log (\lambda_{\rm b} - 1)$, data measured at elevated temperatures do not superpose to yield a single curve. Because of scatter in the experimental data, T_0/T can in practice be omitted when considering the dependence of $\sigma_{\rm b}$ on $\lambda a_{\rm T}$, although the temperature ratio is ordinarily included in conformity with theoretical concepts.

Figure 4 shows data [8, 16] measured on an SBR vulcanizate at various extension rates over an extended temperature range. The data are plotted against —log

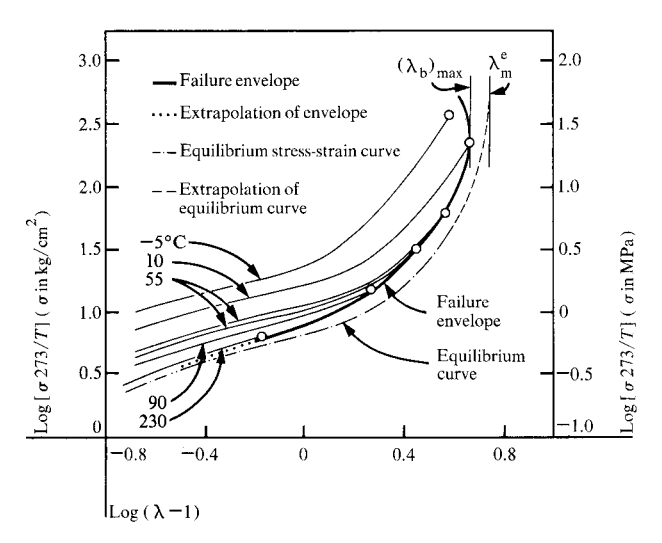


Figure 5 Characteristic features of stress-strain curves and the failure envelope for a fluorohydrocarbon (Viton) rubber vulcanizate [8].

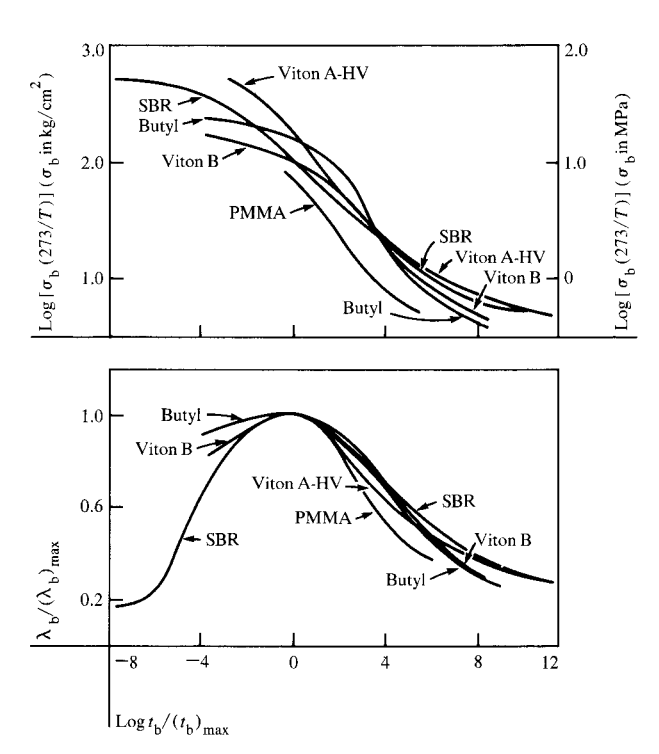


Figure 6 Comparison of the time-dependence of $\sigma_{\rm b}$ and $\lambda_{\rm b}$ for various single-phase noncrystallizable elastomers; $(t_{\rm b})_{\rm max}$ is the reduced time-to-break associated with $(\lambda_{\rm b})_{\rm max}$ [8].

 $\dot{\lambda}a_T$, where the temperature function a_T equals one at $-10^{\circ}\mathrm{C}$ (263 K), the selected reference temperature. Moving from right to left corresponds to an increase in extension rate under isothermal conditions or to a reduc-

tion in temperature, the extension rate being fixed. The upper panel shows that the temperature-reduced tensile strength $\sigma_b 263/T$ varies about 100-fold. With a reduction in the temperature or an increase in extension rate, the ultimate elongation (lower panel) increases from 100 to 600 percent and then drops rapidly. Because of the variation in λ_b , the true stress-at-break $\lambda_b \sigma_b$, based on the cross-section of a deformed specimen, passes through a maximum as shown by the uppermost curve.

Figure 5 shows the failure envelope for VitonTM A-HV, a fluorohydrocarbon elastomer produced by E. I. duPont de Nemours and Company; most of the defining points have been omitted. Also shown are a few stress-strain curves and the (hypothetical) equilibrium curve derived from time-dependent data and the equilibrium modulus [8, 17]. It is seen that the equilibrium curve for this elastomer lies to the right of the failure envelope. For many elastomers, the equilibrium curve and the lower portion of the failure envelope are essentially coincident.

The curves in Fig. 6 were constructed from data obtained on single-phase noncrystallizable elastomers having different glass temperatures and cross-link densities [8]. This figure indicates that the curves representing the ultimate tensile properties of such elastomers are rather similar when data on elastomers in corresponding states are compared and account is taken of the dependence of λ_b on the cross-link density. The latter is accomplished through use of $\lambda_b/(\lambda_b)_{\rm max}$ as the ordinate in the lower panel. The former is achieved by using $t_b/(t_b)_{\rm max}$ as the abscissa, where $(t_b)_{\rm max}$ is the temperature-reduced time-to-break associated with $(\lambda_b)_{\rm max}$. Figure 6, along with the original data, shows that $\sigma_b \lesssim 7~{\rm kg/cm^2}~(0.7~{\rm MPa})$ and $\lambda_b < 2~{\rm for}$ each elastomer at elevated temperatures (e.g., at $T > T_{\rm g} + 100^{\circ}{\rm C}$).

These and other data [8] indicate that all single-phase noncrystallizable elastomers fracture under a small stress at a low elongation, except at low temperatures or high extension rates. Although such elastomers are reasonably tough in some temperature range, the viscous effects at such temperatures are substantial (i.e., the hysteresis is large) and then the materials do not have the elastomeric properties often desired. Also, because strength is imparted primarily by viscoelastic processes, a specimen maintained under constant deformation or constant load commonly fractures after some period.

Polyurethane and poly(urea-urethane) elastomers

When a diisocyanate reacts with a triol or tetrol mixed with a hydroxyl-terminated prepolymer, e.g., poly-(oxypropylene) glycol or poly(oxytetramethylene) glycol, whose molecular weight is approximately 2000, an elastomeric network results. This type of polyurethane elastomer is typically a single-phase copolymer whose glass temperature increases with the concentration of

Figure 7 Structure of hard segments in poly(urea-urethane) and polyurethane elastomers; " ϕ -rings" is the average number of aromatic rings in a hard segment, and W_c is the weight fraction of hard segments in an elastomer.

the diisocyanate moieties, at least when the diisocyanate is toluene diisocyanate or hexamethylene-1, 6-diisocyanate [18-21]. Their ultimate tensile properties are similar to those of the elastomers already discussed, unless the chains crystallize under strain; such polyurethanes thus lack toughness except under special test conditions.

In contrast, a tough elastomer usually results when a diisocyanate is reacted with a hydroxyl-terminated prepolymer and either a short-chain diol (e.g., 1,4-butanediol) or a diamine, giving a block copolymer, typically not cross-linked through primary valence bonds. The diisocyanate and the short-chain diol or diamine form hard segments that segregate into domains which, because of their plastic (non-rubbery) characteristics, serve as physical cross-links and also impart toughness, as previously mentioned. The glass temperature depends primarily on the composition of the soft phase [18, 20, 21].

In recent years, the morphology of such block copolymers in both the isotropic and deformed states has been investigated by various techniques: wide- and small-angle x-ray diffraction [22-28]; infrared and especially infrared dichroism [28-33]; stress birefringence [34, 35]; and low-angle light scattering [28, 36, 37]. These studies show that: a) The plastic phase may be amorphous, paracrystalline, or crystalline; b) the hard and soft segments are often partially intermixed; c) the nature, volume fraction, and perfection of the domains depend on thermal and thermomechanical history; d) in certain instances, the domains form spherulitic super-

structures; and e) when a specimen is highly stretched, the morphology takes on a fibrous texture and, in some instances, the soft segments crystallize. Relations between the structure and properties of polyurethane and poly(urea-urethane) block copolymers are reviewed briefly in Ref. [38].

• Elastomers studied and test methods

The elastomers studied contain the two types of hard segments depicted in Fig. 7. Poly (urea-urethane) elastomers were prepared by reacting Adiprene L-100 (100 parts) with 4,4'-methylene-bis-(2-chloroaniline) (12.5 parts), commonly termed MOCA, at either 100 or 25°C. (Adiprene L-100TM, produced by E. I. du Pont de Nemours and Company, is a viscous liquid, has a molecular weight of about 2000 and is poly(oxytetramethylene) glycol (POTMG) end-capped with toluene diisocyanate.) The weight fraction of the hard segments, W_a , is about 0.26. Low-angle light-scattering patterns [39] showed that the 100°C-cured/(373K), but not the 25°Ccured/(298K), elastomer contains spherulitic superstructures, similar to those found in other poly(ureaurethane) elastomers [28] and also in polyurethanes having piperazine-butanediol hard segments [36, 37]. Emphasis is given here to the 100°C-cured material whose stiffness is somewhat greater, due to the spherulitic superstructures, than for that cured at 25°C.

The polyurethane elastomers, supplied by E. A. Collins of the B. F. Goodrich Chemical Company, were prepared from POTMG, 1,4-butanediol (BD), and 4,4'-

159

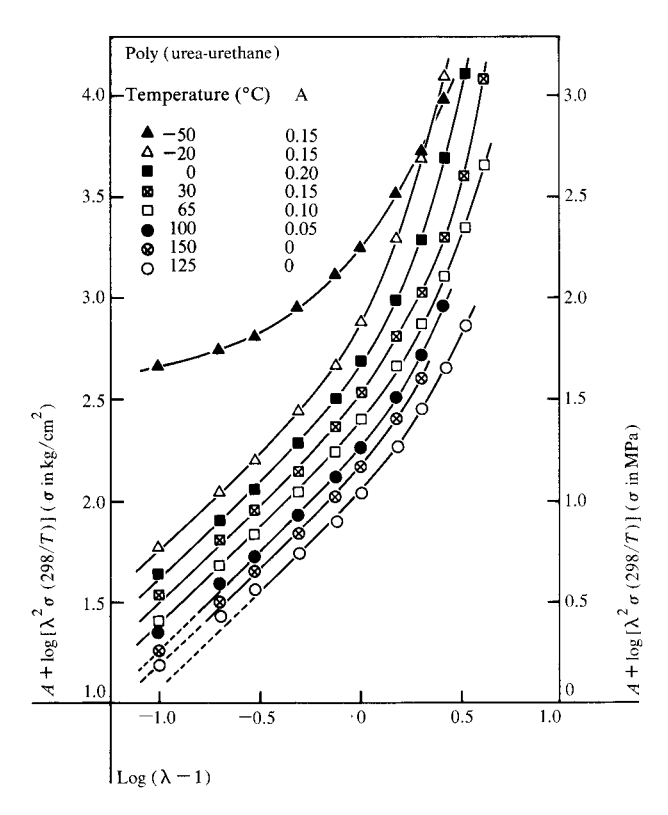


Figure 8 One-minute stress-strain isochrones for poly(ureaurethane) elastomer shown by doubly logarithmic plots of $\lambda^2 \sigma 298/T$ against $(\lambda - 1)$. On the ordinate, A is an arbitrary constant used to separate the curves for clarity.

diphenylmethane diisocyanate (MDI). Their designations, proposed by Cooper who studied such elastomers [29, 31-35], are ET-38-1, ET-38-2, and ET-24-2, indicating that the soft segment is a polyether, the MDI content is either 38 percent or 24 percent, and the molecular weight of the soft segment is either 1000 or 2000. Tabulated in Fig. 7 are the average numbers of butanediol moieties and aromatic rings in each hard segment and also the weight fraction of hard segments.

Some of the hard segments in the polyurethanes undoubtedly reside outside the domains, as indicated by the mechanical loss tangent measured [40] on ET-38-2 and ET-38-1 at 110 Hz as a function of temperature. Upon invoking the well-known WLF equation [2] to account for the frequency dependence of the loss tangent, we find that the glass temperatures of the soft phase in ET-38-2 and ET-38-1 are about -80 (193) and -70° C (203 K), respectively. These values are rather close to -84° C, the dilatometrically determined $T_{\rm g}$ for high molecular weight POTM [41]. On the other hand, it has been reported [40] that the glass temperatures of ET-38-2 and ET-38-1, measured by differential scanning calorimetry (DSC) at an unspecified heating rate, are -70 and -42° C, respectively. A recent study [42] has

shown that $T_{\rm g}$ depends markedly on the thermal history of a specimen and that $T_{\rm g}$ of an annealed sample of 2-ET-38-1, measured by DSC at a heating rate of 20°C per minute, is below -60° C. (2-ET-38-1 has the same composition as ET-38-1 but was prepared by a two-step procedure.)

During the curing of the polyurethane elastomers, some POTMG chains are likely to become directly coupled by single MDI molecules, thus yielding segments that are miscible with the soft phase; these and any isolated hard segments cause $T_{\rm g}$ to be higher than that for POTM. The $T_{\rm g}$ of annealed samples of the polyurethanes is probably no more than 15°C above that for POTM, so the fraction of miscible segments, though significant, is not large.

With an Instron tester, tensile stress-strain curves were measured at various temperatures and crosshead speeds (as indicated in Figs. 10-12) on circular rings cut from sheets of the elastomers about 0.2 cm thick. Only one ring was tested under each set of test conditions. Typically, the inside and outside diameters of a ring were 2.0 and 2.2 cm. For reasons given elsewhere [43], the elongation-at-break was based on the inside diameter of a ring, and the stress-at-break was obtained from the force-extension curve by an extrapolation procedure. In studying ET-38-2 and ET-38-1, the cubic equation [43b] was not used to obtain the elongation-atbreak from the crosshead displacement. From isothermal stress-strain curves measured at various extension rates, the one-minute stress-strain isochrone was derived at each temperature.

• Dependence of stiffness on temperature

When a single-phase elastomer is subjected to a tensile deformation that increases in direct proportion to the time, the stress-time response at a particular temperature can usually be represented by [10, 12, 44]

$$\lambda \sigma(t, \lambda) = E_{cr}(t) \Gamma(\lambda), \tag{1}$$

where $\lambda \sigma$ is the true stress (based on the cross-section of the deformed specimen), $E_{\rm cr}(t)$ is a time-dependent parameter termed the constant-strain-rate modulus in tension (denoted by F(t) in Ref. [44]), and $\Gamma(\lambda)$ is a function solely of the extension ratio λ ; the latter equals $\lambda t + 1$, where again λ is the constant rate of extension. Equation (1) is usually valid, provided the test temperature is not too low and λ is not unduly large [10, 12]. Generally, $\Gamma(\lambda) \approx \lambda - 1$ when $1 < \lambda \lesssim 2$, i.e., at extensions up to 100 percent. Then $\lambda \sigma/(\lambda - 1)$ evaluated from a stress-strain isochrone (for which $t = t^*$) is independent of λ and equals the modulus $E_{\rm cr}(t^*)$.

For the poly(urea-urethane) and the polyurethane elastomers, as well as other two-phase elastomers [45], the ratio $\lambda \sigma / (\lambda - 1)$ is not only time dependent but

also depends strongly on λ , even at small deformations. The plots of $\log \lambda^2 \sigma 298/T$ vs $\log (\lambda - 1)$ in Fig. 8 show one-minute stress-strain data (i.e., $t^* = 1$ min) on the 110°C -cured poly (urea-urethane) elastomer at temperatures from -50 to 150°C (223 to 323 K). (The temperature ratio 298/T has no significance here.) The straight segments of the curves have a unity slope. Except at -50 and at 100°C and above, these segments represent the data reasonably well for $1.1 < \lambda \lesssim 2$. (Although the data at all temperatures between -20 and -150°C can be represented more precisely by a different relation between stress and strain [45], the empirical representation in Fig. 8 is adequate for present purposes.) It thus follows that

$$\lambda \sigma / (\lambda - 1) = k(T) / \lambda$$
 for $1.1 \lesssim \lambda \lesssim 2$. (2)

where k(T) is a temperature-dependent parameter and $k(T)/\lambda$ can be viewed as a strain-dependent modulus (hereafter called the secant modulus). This modulus was thus derived at $\lambda=1.38$ and is plotted logarithmically against the temperature in Fig. 9, which also shows data on the three polyurethane elastomers. (When the ratio $\lambda\sigma/(\lambda-1)$ is independent of deformation, it is the time-dependent modulus $E_{\rm cr}(t)$; otherwise it is a time-dependent secant modulus, which can be used as a measure of stiffness.)

Figure 9 shows that the secant modulus for the poly-(urea-urethane) elastomer is virtually temperature independent between 0 and 160°C (273 and 433 K). As shown elsewhere [45], this modulus increases with a reduction in strain and its temperature coefficient becomes positive at small strains. The latter behavior is also shown [45] by the storage modulus measured at 11 Hz under infinitesimal strain. It was found that the poly (ureaurethane) elastomer dissolved in dimethylformamide during 14 days, which indicates that the polymer was not cross-linked by primary valence bonds.

The small temperature coefficient of the storage and secant moduli, which is quite unusual for an elastomeric block copolymer, indicates that the urea-urethane domains are highly stable, that chain mobility in the soft phase is high even at 0°C, and that the domains reorient rapidly in a stressed specimen. The rate of stress relaxation is small [45], being about 3 percent per decade of time from 30°C, or lower, up to 150°C. The high stability of the domains undoubtedly results because the urea groups [46] impart high cohesive energy, and thus a high melting point, to the domains which probably are crystalline, or paracrystalline, as reported [28] for other poly(urea-urethane) elastomers. Although the melting or softening temperature of domains is not known, the data in Fig. 9 indicate that it is above 150°C. A high melting temperature should cause phase separation to be essentially complete, provided the material is in thermo-

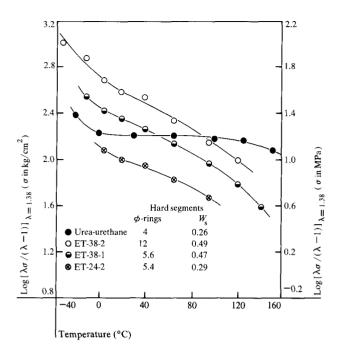


Figure 9 Semilogarithmic plots showing the temperature dependence of $\lambda \sigma / (\lambda - 1)$ evaluated at $\lambda = 1.38$ from one-minute stress-strain isochrones.

dynamic equilibrium, or nearly so. In line with these observations, x-ray studies show that short urea-ure-thane segments aggregate readily [25], but that the hard segments in a polyurethane form domains [22] only when each segment contains more than one butanediol moiety.

The secant modulus of each polyurethane elastomer differs markedly (Fig. 9) and exhibits a large, yet similar, temperature dependence. (For ET-38-1, the relaxation rate is about 12 percent per decade of time, substantially greater than the 3 percent found for the poly-(urea-urethane) elastomer [45].) Infrared dichroic measurements [32, 33] on ET-38-1 under an elongation of 150 percent have shown that the orientation of the hard segments and the disorientation of the soft segments are time dependent, whereas the response of the segments in ET-38-2 is essentially time independent. Thus, the domain orientation and relaxation processes are quite different in these two materials.

The hard segments in ET-38-2 are exceptionally long; each contains, on the average, 12 aromatic rings and 5 butanediol moieties. The segments form large crystalline domains [32] that impart opacity to the material. With a progressive increase in elongation, the segments in domains first become oriented perpendicular (negative orientation) and then parallel (positive orientation) to the stretch direction. The latter process necessitates disruption and reorganization of domains at high elonga-

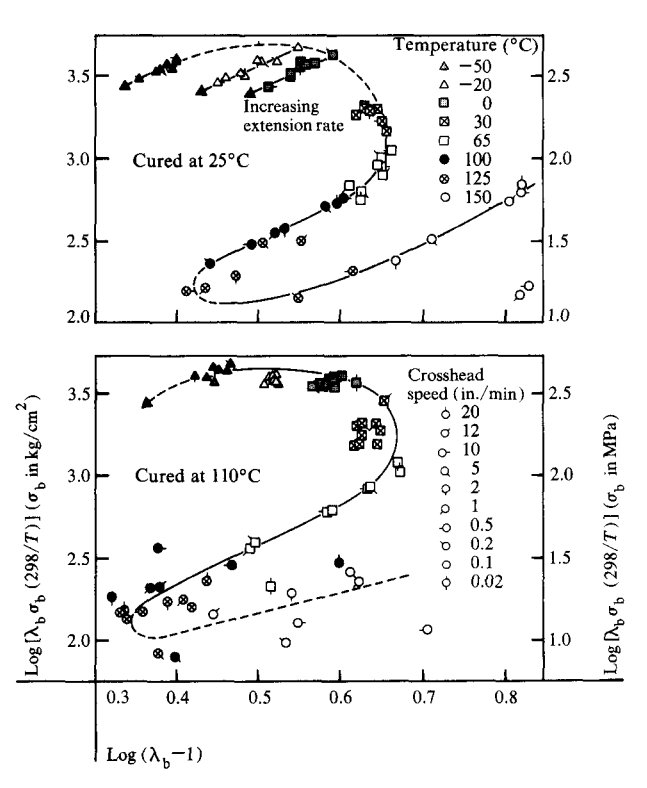


Figure 10 Doubly logarithmic plots of $298\lambda_b\sigma_b/T$ against (λ_b-1) for poly(urea-urethane) elastomers cured at 25°C (298 K) (upper panel) and at 100°C (383 K) (lower panel) [18].

tions [32, 33]. In contrast, the segments in the normally noncrystalline domains in ET-38-1 orient into the stretch direction at all elongations. During the stretching of ET-38-1 and ET-38-2, and probably ET-24-2 also, the domains may form an interlocking structure because of asymmetry and high concentration, as discussed in Ref. [33]. The time-independent response of the domains in ET-38-2 undoubtedly results because the domains are quite rigid and form an interlocking structure when a specimen is stretched. Unless the domains can continuously deform, re-orient, or be disrupted, little relaxation can occur.

Among the polyurethanes, ET-24-2 has the lowest secant modulus (Fig. 9). This undoubtedly occurs because the concentration of hard segments is the lowest, although other relevant factors are the completeness of phase separation [42] and the morphology, rigidity, and ductility of the domains. The concentrations of the hard segments in ET-38-1 and ET-38-2 are similar, yet their secant moduli differ and also depend on strain magnitude. While domain ductility and interfacial layers containing both hard and soft segments may be responsible for the dependence on strain magnitude, the modulus under infinitesimal strain should depend only on the rigidity and morphology of domains. (The shape of crys-

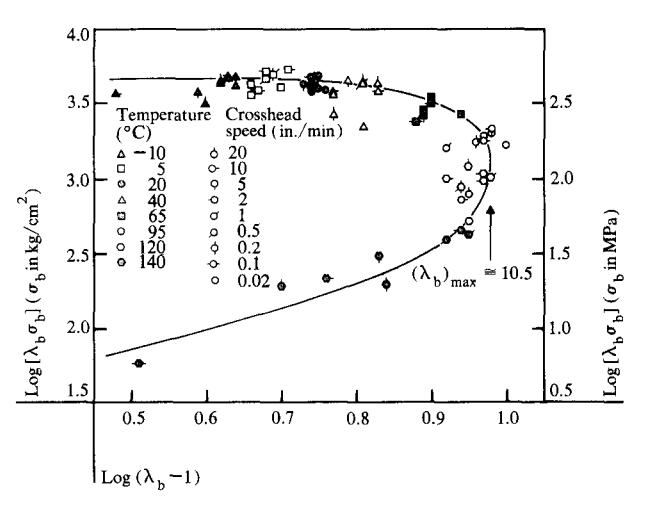


Figure 11 Doubly logarithmic plot of $\lambda_b\sigma_b$ against (λ_b-1) for polyurethane elastomer ET-38-1.

tallites is known to affect strongly the modulus of a semicrystalline polymer [47].) Because the storage moduli (infinitesimal strain) of ET-38-1 and ET-38-2 are markedly different and the temperature dependence of the modulus for each is similar to that shown in Fig. 9 [40], it appears that the substantial decrease in the modulus with temperature results from a progressive softening of the domains and also from an increase in the degree of mixing of hard and soft segments [42].

• Strength and extensibility

As previously mentioned, fracture involves the formation of a microcrack that grows slowly to some critical size; high-speed propagation then ensues. In block copolymers, the plastic domains can effectively impede the formation and slow growth of microcracks. For a crack of significant size to develop and propagate, domains must be disrupted, a process necessitating considerable energy. Prior to macroscopic failure, several beneficial processes can occur: 1) Domains can deform in localized regions under high stress, thereby diminishing the stress so that microcracks do not form or crack-arrest is effected; 2) domain morphology can change during the imposition of a large deformation and produce an oriented fibrous texture that inherently is strong in the orientation direction; and 3) the soft matrix may undergo strain-induced crystallization, thus generating plastic domains that impart strength. In addition, the reduced mobility of the soft segments at a low temperature can augment strength. These concepts provide a qualitative explanation of the strength of elastomeric block copolymers.

Data determined at various extension rates and temperatures on the poly(urea-urethane) and polyurethane

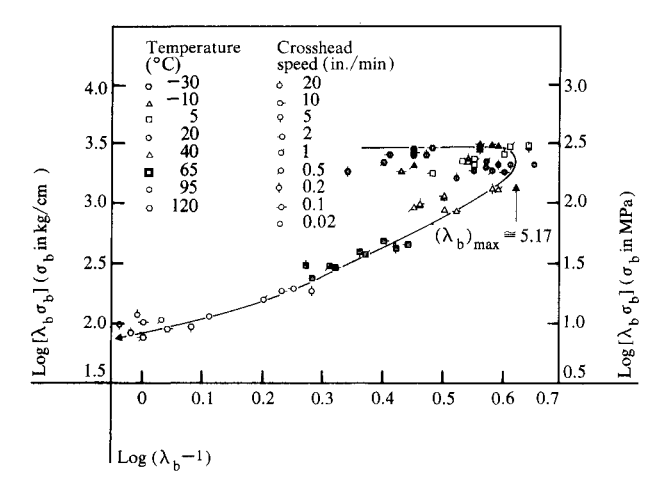


Figure 12 Doubly logarithmic plot of $\lambda_b \sigma_b$ against $(\lambda_b - 1)$ for polyurethane elastomer ET-38-2.

elastomers are shown in Figs. 10 – 12 by the plots of true stress-at-break vs strain-at-break on doubly logarithmic coordinates. (A similar representation of data of ET-24-2 appears in Ref. [18].) Because various molecular and supermolecular processes occur during the stretching of these elastomers, time-temperature superposition is inapplicable. Therefore Figs. 10-12 cannot be interpreted as directly and simply as similar representations of data on single-phase noncrystallizable elastomers. Nevertheless, the plots show clearly that the ultimate tensile properties depend markedly on temperature and extension rate. (Other conclusions about the poly(urea-urethane) and ET-24-2 are presented in Ref. [18].) By interpolation of data at various extension rates, $\lambda_b \sigma_b$ and $(\lambda_b - 1)$ were evaluated at $d\lambda/dt = 1 \text{ min}^{-1}$ and are plotted against temperature in Fig. 13. Data on the 25°C-cured poly-(urea-urethane), shown elsewhere [18], are qualitatively similar to those on the 110°C-cured material.

Aspects of the results in Fig. 13 are clarified upon recognizing that these elastomers are uncross-linked and can undergo viscous flow, especially at elevated temperatures. That is, domain morphology can be changed such that elastic recovery will not be complete. Thus, broken specimens of ET-38-1 and ET-38-2 were heated for 20 hours at 60°C and their lengths then measured. The lower panel in Fig. 14 shows the temperature dependence of $[(\lambda_b/\lambda_r)-1]$, a measure of the recoverable deformation. The ratio λ_b/λ_r equals L_b/L_r , where L_b and L_r are the lengths of a specimen at the instant of fracture and after recovery, respectively. Since both L_b and L_r depend on the extension rate, λ_b/λ_r was evaluated at an extension rate of 1 min⁻¹ by interpolation of data from tests at different rates.

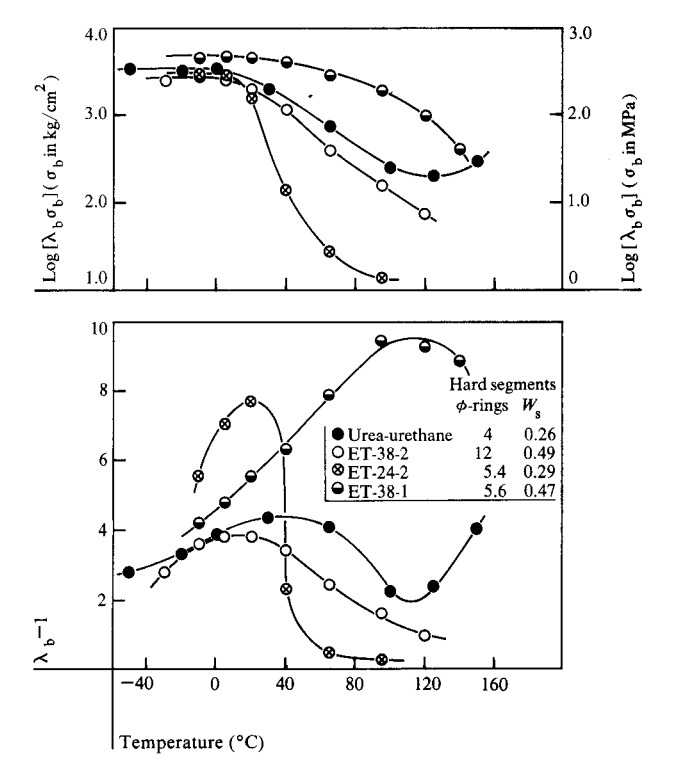


Figure 13 Plots of $\log \lambda_b \sigma_b$ (upper panel) and $(\lambda_b - 1)$ (lower panel) against temperature. Data were evaluated at an extension rate of 1 min⁻¹ and are for poly(urea-urethane) and polyurethane elastomers.

A comparison of the curves in the upper and lower panels of Fig. 14 shows that the permanent deformation of ET-38-1 is large at elevated temperatures; it increases from 20 percent at -10°C to 230 percent at 95°C. In contrast, the permanent deformation for ET-38-2 is 70 to 80 percent at and below 20°C; with a temperature increase, it decreases and becomes 20 percent at 95°C. For both elastomers, $[(\lambda_b/\lambda_r)-1]$ passes through a maximum at 20 to 40°C. Thus, the temperature dependence of $[(\lambda_b/\lambda_r)-1]$, even when the permanent deformation is large at elevated temperatures, resembles that of (λ_b-1) for an elastomer that flows little at high temperatures. Interestingly, $[(\lambda_b/\lambda_r)-1]$ for ET-38-1 is similar to (λ_b-1) for the poly(urea-urethane) elastomer (Fig. 13); for the latter, λ_b/λ_r was not determined.

For the softest polyurethane, ET-24-2, both $\lambda_b \sigma_b$ and $(\lambda_b - 1)$ are very low above 40°C (Fig. 13). Presumably, the domains are soft and lack sufficient cohesive strength to retard crack growth, yet they inhibit viscous flow. Below 40°C, the increased toughness of the domains in combination with the higher viscosity of the soft matrix impart sufficient strength so that a specimen can be stretched until reinforcement by strain-induced crystallization comes into play [18]. The occurrence of

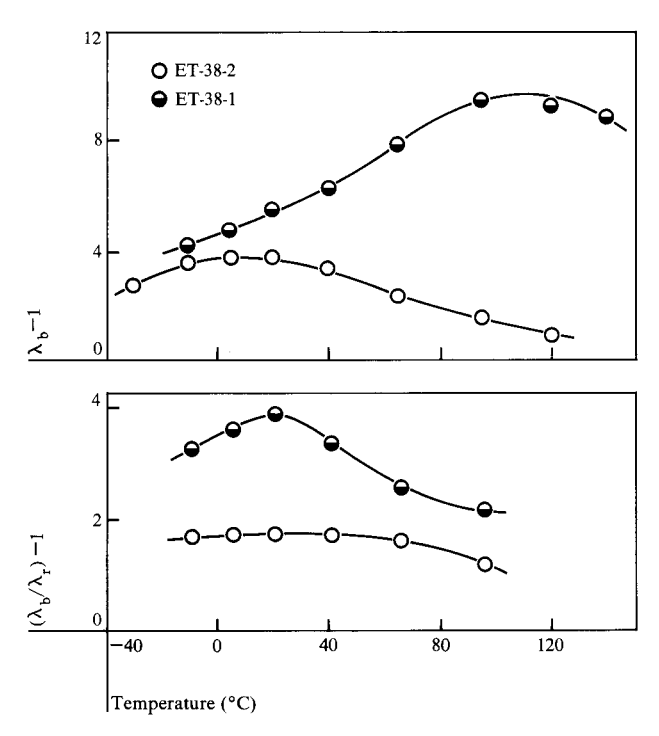


Figure 14 Data on polyurethane elastomers evaluated at an extension rate of 1 min^{-1} . Upper panel shows $(\lambda_b - 1)$, reproduced from Fig. 13. Lower panel shows $[(\lambda_b/\lambda_r) - 1]$ where $\lambda_b/\lambda_r = L_b/L_r$, L_b and L_r being the lengths of a specimen at the instant of fracture and after elastic recovery, respectively.

crystallization was verified by low-angle light-scattering measurements on a specimen stretched at room temperature [39].

The open circles in Fig. 13 represent data on the stiffest polyurethane, ET-38-2. Its domains, which are partially crystalline and melt above 200°C (473 K) [32, 33, 40, 48, 49], impede flow rather effectively at high temperatures (Fig. 14). The low extensibility, especially at high temperatures, occurs possibly because the relatively large, rigid domains form a gross interlocking structure [33]. (Elastomers are not strengthened by large filler particles.) The high extensibility of ET-38-1, a sizable fraction of which is not recoverable (Fig. 14), results because the domains are smaller and more deformable than those in ET-38-2. The domain characteristics are such that fracture processes are nullified initially, allowing a highly oriented fibrous structure to develop which fractures under a very high stress. Except below 10°C, ET-38-1 is markedly stronger than the other elastomers (cf. the upper panel of Fig. 13). In contrast to the polyurethanes, the poly(urea-urethane) becomes stronger and more extensible above 120°C (393 K) because the domains, now being more deformable, can reorganize into a more fibrous structure than is possible near 100°C.

As previously mentioned, the soft POTM matrix in ET-24-2 crystallizes under strain below about 40°C, thereby imparting strength. If the POTM matrix in the other elastomers (Fig. 13) does in fact crystallize when specimens are stretched under certain conditions, the strength is affected only marginally by the strain-induced generation of crystalline domains. (Quite possibly, the matrix does crystallize under certain conditions [22, 28, 50].) Although strain-induced crystallization can occur far above 38°C, the melting point of isotropically crystallized POTM [41], the high strength of the poly(urea-urethane) and ET-38-1 elastomers at the highest test temperatures undoubtedly does not result from strain-induced crystallization. Poly(urea-urethane) elastomers similar to those considered here have been prepared [51] from poly(oxypropylene) glycol (PPG), MOCA, and TDI. The PPG segments cannot crystallize, and yet the strength of such an elastomer is high at room temperature, so the high strength of the poly(ureaurethane) elastomer (Fig. 13) cannot be attributed primarily to crystallization of POTM chains.

Strength of other block copolymers

In Fig. 15, $\lambda_b \sigma_b$ for various segmented and triblock elastomeric copolymers is plotted against the weight fraction of the hard segments. Except where noted, the data are at 25°C. (Data for the lines without points are presented in Ref. [18].) The lowest curve represents data on cross-linked polyurethane elastomers, prepared from poly(oxypropylene) glycol, dipropylene glycol, a triol, and TDI [19]. These elastomers lack strength because they do not contain plastic domains [18]. Elimination of the triol and replacement of the dipropylene glycol with toluene-2,4-diamine gives poly(urea-urethane) elastomers [20], designated PPG-TDA-TDI, that contain plastic domains which impart considerable strength. With minor exceptions, the triblock elastomers (SBS, styrene-butadiene-styrene; SIS, styrene-isoprene-styrene; mSImS, α -methylstyrene-isoprene- α -methylstyrene), the segmented polysiloxane-polycarbonate copolymers, and the Adiprene elastomers, which are similar to the poly-(urea-urethane) discussed here, have a true stress-atbreak that is independent of the hard-segment content; presumably this is no longer true when $W_{\rm s} < 0.20$. (Values of $\lambda_b \sigma_b$ were computed from data given by Morton and Fetters [52, 53] on the triblock elastomers, by Vaughn [54] on the segmented siloxane-carbonate copolymers, and in E. I. du Pont de Nemours and Company trade literature on the Adiprene elastomers.) The differences in the strengths of the domain-containing copolymers for which $W_s > 0.20$ are considered elsewhere [18] in terms of the characteristics of the domains and the soft rubbery matrix.

It may be concluded from Fig. 15 that the true stress-at-break is large for most block copolymers and, for a particular type, is independent of domain concentration provided $W_s \gtrsim 0.20$. Accordingly, $\lambda_b \sigma_b$ for the poly-(urea-urethane) and polyurethane elastomers at 25°C (Fig. 13) is similar to that represented by the Adiprene line in Fig. 15. Typically, the ultimate elongation for a particular type of block copolymer decreases with an increase in domain concentration. Therefore, whenever $\lambda_b \sigma_b$ is independent of domain concentration, the nominal tensile strength σ_b (the quantity usually reported in the literature) decreases with domain concentration.

Summary

All undiluted polymers composed of flexible macromolecules exhibit rubberlike properties to some degree, except when long-range molecular rearrangements are precluded by low mobility of polymeric segments. For a single-phase noncrystallizable elastomer, tensile stressstrain curves depend on temperature and extension rate (or time), owing to effects imparted by segmental mobility. When a specimen is deformed substantially, microcracks form and grow slowly until a crack becomes unstable and propagates catastrophically. The rate of slow growth depends on the dissipation of elastic energy through viscoelastic processes near the tip of a growing crack. Because this process is ineffective except when mobility is relatively low, and yet represents an important source of strength in single-phase noncrystallizable elastomers, such materials lack toughness.

The contribution of the network per se to strength has been discussed by Gent [55]. In the complete absence of viscous effects, σ_b has been estimated [55, 56] to be between about 5 and 9 kg/cm² (0.5 and 0.9 MPa), dependent *inter alia* on the molecular weight of effective network chains and their concentration.

Toughness necessitates a dispersed phase, either colloidal particulate filler, innate plastic domains, or domains resulting from strain-induced crystallization. The effect of innate plastic domains on mechanical properties was considered in terms of data on poly(urea-urethane) and polyurethane elastomeric block copolymers. The hard segments in the poly(urea-urethane) elastomers, though relatively short, aggregate into domains that are quite rigid because the cohesive energy of the urea-urethane segments is high. Because of domain rigidity, among other things, the secant modulus (evaluated from stress-strain isochrones at extensions greater than 10 percent) is nearly temperature independent from about 0 to 120°C; viscoelastic processes in the soft matrix are inconsequential, and the domains reorient readily under stress. In contrast, the hard segments in the polyurethane elastomers contain butanediol moieties and have a low cohesive energy. The domains appear to be rather

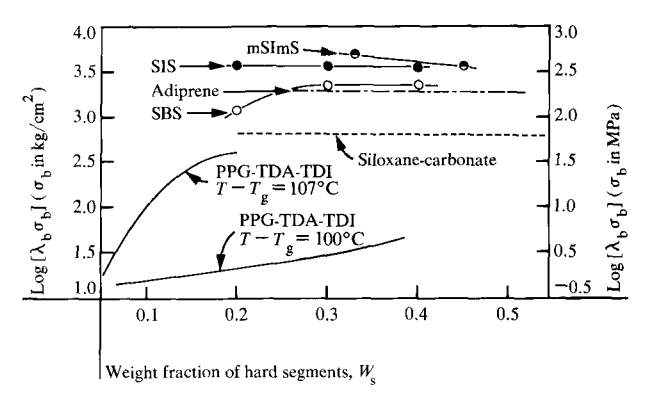


Figure 15 Dependence of true stress-at-break on the weight fraction of domain-forming segments in various segmented and triblock elastomers. Lowest curve is for polyurethane elastomers whose polar segments do not form domains. Except where indicated, data were determined at 25°C (298 K) [18].

deformable and to soften progressively with increasing temperature. Such characteristics, along with some increase in the degree of mixing of hard and soft segments, presumably cause the secant modulus to depend substantially on temperature.

The effectiveness of domains for imparting toughness depends on their concentration, mechanical characteristics, and morphology. Toughness results because the development of a microcrack to a critical size necessitates the deformation and disruption of domains and thus the expenditure of considerable energy. Also, plastic deformation of domains can forestall crack formation and growth, enabling a specimen to be highly stretched and the domains to be transformed into an oriented fibrous structure that is inherently tough in the orientation direction.

When domains have certain characteristics, only a high concentration gives high toughness. The hard segments in ET-38-1 and ET-24-2 are ostensibly identical, but the ultimate tensile properties of these elastomers are grossly different above 40°C. Below 40°C, the toughness of ET-24-2 results from domains generated by strain-induced crystallization. The concentration of domains in ET-24-2 ($W_s = 0.29$) is too low to impede crack growth above 40°C, but viscous flow is prevented. In contrast, ET-38-1 for which $W_s = 0.47$ can be highly stretched, especially at elevated temperatures at which a sizable fraction of the deformation is not recoverable. The resulting fibrous structure imparts an exceptionally large true stress-at-break at elevated temperatures.

The concentration of domains in ET-38-1 and ET-38-2 is essentially identical ($W_{\rm s}=0.47$ and 0.49, respectively), yet their ultimate tensile properties differ markedly owing to the dissimilar physical characteristics of the domains. The hard segments in ET-38-2 are long. The domains, which are crystalline or partially so, are

very large and do not deform readily. They not only impede viscous flow at elevated temperatures but seemingly also promote fracture.

The poly(urea-urethane) elastomer is tough over a broad temperature range because the high cohesive energy of the hard segments imparts rigidity and stability to the domains. The small size of the domains, compared with those in ET-38-2, is also beneficial. The marked differences in the properties of the poly(urea-urethane) and ET-24-2, both of which have nearly the same hard-segment content, illustrates the importance of domain characteristics. Nevertheless, in spite of differences in domain characteristics and concentrations, values of $\lambda_b \sigma_b$ below 20°C for the poly(urea-urethane) and polyurethanes studied are high and have similar magnitudes, being in the range 3600 \pm 100 kg/cm² (360 \pm 10 MPa).

Acknowledgments

The tensile data on the polyurethane and poly(ureaurethane) elastomers were determined by R. D. Diller, who also prepared the latter. The polyurethane elastomers were supplied by E. A. Collins of the B. F. Goodrich Chemical Company Technical Center, Avon Lake, Ohio.

References

- 1. A. V. Tobolsky, *Properties and Structures of Polymers*, John Wiley & Sons, Inc., New York, 1960.
- J. D. Ferry, Viscoelastic Properties of Polymers, 2nd ed., John Wiley & Sons, Inc., New York, 1970.
- L. R. G. Treloar, The Physics of Rubber Elasticity, 2nd ed., Oxford University Press (Clarendon), London and New York, 1958.
- L. R. G. Treloar, Rep. Prog. Phys. 36, 755 (1973); reprinted in Rubber Chem. Technol. 47, 625 (1974).
- T. L. Smith, Treatise on Materials Science and Technology, Vol. 10, J. M. Schultz, ed., Academic Press, Inc., in publication.
- L. Bateman, C. G. Moore, M. Porter, and B. Saville, The Chemistry and Physics of Rubberlike Substances, L. Bateman, ed., John Wiley & Sons, Inc., New York, 1963, Chapter 15.
- Pertinent discussions are contained in J. Polymer Sci. (Part C) 26 (1969); Block Polymers, S. L. Aggarwal, ed., Plenum Press, Inc., New York, 1970; Colloidal and Morphological Behavior of Block and Graft Copolymers, G. E. Molau, ed., Plenum Press, Inc., New York, 1971; and Block Copolymers, D. C. Allport and W. H. Janes, eds., John Wiley & Sons, Inc., New York, 1973.
- T. L. Smith, Rheology, Vol. V, F. R. Eirich, ed., Academic Press, Inc., New York, 1969, Chapter 4.
- 9. J. C. Halpin, J. Appl. Phys. 36, 2975 (1965).
- T. L. Smith and R. A. Dickie, J. Polymer Sci. (Part A-2)
 7, 635 (1969).
- 11. R. A. Dickie and T. L. Smith, *Trans. Soc. Rheol.* 15, 91 (1971)
- T. L. Smith, in Mechanical Behavior of Materials (Proc. Int. Conf. Mech. Behavior Materials), Vol. III, The Society of Materials Science, Kyoto, Japan, 1972, p. 431.
- 13. J. C. Halpin, Rubber Chem. Technol. 38, 1007 (1965).
- 14. J. C. Halpin, J. Appl. Phys. 35, 3133 (1964).
- J. C. Halpin and H. W. Polley, J. Compos. Mater. 1, 65 (1967).

- 16. T. L. Smith, J. Polymer Sci. 32, 99 (1958).
- T. L. Smith and J. E. Frederick, J. Appl. Phys. 36, 2996 (1965).
- 18. T. L. Smith, J. Polymer Sci., Polymer Phys. Ed. 12, 1825 (1974).
- T. L. Smith and A. B. Magnusson, J. Polymer Sci. 42, 391 (1960).
- 20. A. J. Havlik and T. L. Smith, J. Polymer Sci. (Part A) 2, 539 (1964).
- N. S. Schneider, C. S. P. Sung, R. W. Matton, and J. L. Illinger, Macromolecules 8, 62 (1975).
- S. B. Clough, N. S. Schneider, and A. O. King, J. Macromol. Sci. - Phys. 2, 641 (1968).
- 23. R. Bonart, J. Macromol. Sci. Phys. 2, 115 (1968).
- 24. R. Bonart, L. Morbitzer, and G. Hentze, J. Macromol. Sci. Phys. 3, 337 (1969).
- 25. R. Bonart, L. Morbitzer, and E. H. Müller, *J. Macromol. Sci.-Phys.* **9**, 447 (1974).
- R. Bonart and E. H. Müller, J. Macromol. Sci. Phys. 10, 177 and 345 (1974).
- C. E. Wilkes and C. S. Yusek, J. Macromol. Sci. Phys. 7, 157 (1973).
- 28. I. Kimura, H. Ishidara, H. Ono, N. Yoshihara, S. Nomura, and H. Kawai, *Macromolecules* 7, 335 (1974).
- R. W. Seymour, G. M. Estes, and S. L. Cooper, *Macro-molecules* 3, 579 (1970).
- C. S. P. Sung and N. S. Schneider, Macromolecules 8, 68 (1975).
- 31. G. M. Estes, R. W. Seymour, and S. L. Cooper, Macro-molecules 4, 452 (1971).
- 32. R. W. Seymour, A. E. Allegrezza, and S. L. Cooper, *Macromolecules* 6, 896 (1973).
- 33. R. W. Seymour and S. L. Cooper, Rubber Chem. Technol. 47, 19 (1974).
- G. M. Estes, R. W. Seymour, D. S. Huh, and S. L. Cooper, *Polymer Eng. Sci.* 9, 383 (1969).
- G. M. Estes, D. S. Huh, and S. L. Cooper, in *Block Polymers*, S. L. Aggarwal, ed., Plenum Press, Inc., New York, 1970, p. 225.
- S. L. Samuels and G. L. Wilkes, J. Polymer Sci. (Part C) 43, 149 (1973).
- G. L. Wilkes, S. L. Samuels, and R. Crystal, J. Macromol. Sci. - Phys. 10, 203 (1974).
- D. C. Allport and A. A. Mohajer, in *Block Copolymers*,
 D. C. Allport and W. H. Janes, eds., John Wiley & Sons,
 Inc., New York, 1973.
- 39. W. H. Chu, IBM Research Laboratory, San Jose, CA, private communication, March 1973.
- D. S. Huh and S. L. Cooper, Polymer Eng. Sci. 11, 369 (1971).
- 41. R. E. Wetton and G. Allen, Polymer 7, 331 (1966).
- 42. G. L. Wilkes and R. Wildnauer, J. Appl. Phys. 46, 4148 (1975).
- 43. T. L. Smith, (a) J. Appl. Phys. 35, 27 (1964); (b) J. Polymer Sci. (Part C) 16, 841 (1967).
- 44. T. L. Smith, Trans. Soc. Rheol. 6, 61 (1962); ibid. 20, 103 (1976).
- 45. T. L. Smith, Polymer Preprints 17, 201 (1976).
- 46. R. Hill and E. E. Walker, J. Polymer Sci. 3, 609 (1948).
- J. C. Halpin and J. L. Kardos, J. Appl. Phys. 43, 2235 (1972).
- 48. R. W. Seymour and S. L. Cooper, Macromolecules 6, 48 (1973).
- W. J. MacKnight, M. Yang, and T. Kajiyama, Polymer Preprints, 9, 860 (1968); also in Analytical Chemistry, R. S. Porter and J. F. Johnson, eds., Plenum Press, Inc., New York, 1968, p. 99.
- S. B. Clough and N. S. Schneider, J. Macromol. Sci. Phys. 2, 553 (1968).
- 51. S. L. Axelrood and K. C. Frisch, Rubber Age 88, 465 (1960).

T. L. SMITH

- 52. M. Morton, Advances in Chemistry Series, No. 99, R. F. Gould, ed., Am. Chem. Soc. Pub., Washington, D.C., 1971, p. 490.
- 53. L. J. Fetters and M. Morton, Macromolecules 2, 453 (1969).
- 54. H. A. Vaughn, J. Polymer Sci. (Part B) 7, 569 (1969).
- 55. A. N. Gent, in Rubber Technology, Vol. 2, F. R. Eirich,
 A. M. Gessler, and H. C. Remsberg, eds., Academic Press,
 Inc., New York; in preparation.

56. T. L. Smith, submitted to Polymer Eng. Sci.

Received July 21, 1976

The author is located at the IBM Research Division laboratory, 5600 Cottle Road, San Jose, California 95193.